Hydro-mechanical path dependency of claystone/bentonite mixture samples characterized by different initial dry densities

M. Middelhoff, Olivier Cuisinier, F. Masrouri, J. Talandier

Hydro-mechanical path dependency of claystone/ bentonite-mixture samples characterized by different initial dry densities

M. Middelhoff [1, 2]*, O. Cuisinier [1], F. Masrouri [1], J. Talandier [2]

[1] Université de Lorraine – LEMTA, UMR 7563 CNRS,
(2 Rue du Doyen Marcel Roubault - BP 10162, 54000 Nancy CEDEX, France)

[2] Agence nationale pour la gestion des déchets radioactifs (Andra), Châtenay-Malabry, France

Olivier.Cuisinier@univ-lorraine.fr

Abstract: In the context of the French Cigéo-project, a mixture composed of 70% processed Callovo-Oxfordian claystone spoil and 30% MX80-bentonite could be a potential backfill material, whose installation aims to stabilize the surrounding rock formation and to limit the propagation of the excavation damaged zone. The backfill material must sustain the overburden pressure, despite it might be exposed to different hydraulic and mechanical paths. The reference concept considers employing conventional compaction techniques, although their employment involves spatial variations in the dry density after compaction. In general, as the initial dry density has a significant impact on the hydro-mechanical behavior of backfill materials, it is of major importance to relate the variations in the initial dry density to differences in the behavior. This experimental laboratory study aimed to analyze how variations in the initial dry density affects the swelling and compression behavior of the claystone/ bentonite-mixture, in particular in unsaturated state. Further, it evaluated whether those variations affected possible hydro-mechanical path dependences. The experimental program comprised suction-controlled oedometer and constant-volume swelling pressure experiments, in which samples characterized by different initial dry densities were exposed to different hydro-mechanical paths. The analysis of microstructural and water retention characteristics complemented the program. Major results indicated that the magnitude of swelling pressure at a given suction depends considerably on the initial dry density, but it is independent of the imposed hydro-mechanical path. Interestingly, the dependency of the yield behavior on the hydro-mechanical path appears to be more pronounced as the initial dry density increases.

Keywords: Callovo-Oxfordian claystone, MX80-bentonite, Microstructure, Water retention curve, Hydro-mechanical behavior, Hydro-mechanical load path dependency

Acknowledgements: The authors gratefully thank Dr. N. Conil of Ineris (formerly contracted by Andra) and Dr. G. Armand of Andra for fruitful discussions that helped to improve this article. Also, the authors thank Dr. S. Gaboreau of BRGM with regard to the performance of microstructural analyses, and Mr. J. Tisot, of LEMTA with regard to the monitoring of swelling pressure and oedometer experiments.

1

1 Introduction

In the context of the French Cigéo-project, different materials are studied as to whether they could be employed to backfill drifts and shafts of the future repository for radioactive waste located at a depth of approximately 500 m in the clay-rich Callovo-Oxfordian sedimentary rock formation, henceforth referred to as Callovo-Oxfordian (COX) claystone formation [5]. The installation of backfill aims to stabilize the surrounding rock formation and to limit the propagation of the excavation damaged zone (EDZ) that arises from the excavation of drifts and shafts and lowers the integrity of the repository system. The backfill must thus exhibit such a swelling pressure and compressibility that it sustains the overburden pressure upon terminating the closure phase. As depicted in Fig. 1, the backfill might undergo different combinations of hydraulic and mechanical paths. The path A – C (– D) describes a possible case of (stepwise) backfill material saturation under constant-volume conditions. It might be followed by loading through the overburden pressure, whose onset occurs once convergence processes cause the partial degradation of the concrete lining. Under laboratory conditions, the path A – C corresponds to the path imposed in constant-volume swelling pressure experiments, whereas path A – B – C – D is imposed in oedometer experiments.

A potential backfill material is a mixture composed of processed Callovo-Oxfordian claystone spoil and MX80-bentonite, whose dominant mineralogical constituents are phyllosilicates (e.g. smectites, illite, illite/ smectite mixed layer minerals) [7, 21]. Since conventional compaction techniques are presumably employed to compact it to the maximum dry density at the optimum water content in situ, the material is initially characterized by a degree of saturation greater than 80% and low suctions. The initial dry density determines not only the hydro-mechanical behavior of smectite-containing materials, but also their microstructural and water retention characteristics [e.g. 1]. It is thus of major interest to analyze how variations in the initial

dry density affect the behavior of such materials upon imposing different hydraulic and mechanical paths and their combinations.

In general, there is a wealth of studies aiming to analyze the microstructural and water retention characteristics and volume-change behavior of smectite-containing materials, in particular in unsaturated conditions [15, 19, 23, 27, 34, 36].

Unsaturated smectite-containing materials are characterized by micro- and macropores, referring to pores between clay aggregates and soil aggregates, respectively. Mechanical and hydraulic loads affect differently those pore populations. Densification reduces only the amount of macropores, whereas the amount of micropores remains stable [e.g. 37]. Hydration affects both pore populations as the amount of micropores increases and the amount of macropores decreases due to the swelling of smectite particles [e.g. 27].

The structure determines the water retention characteristics of smectite-containing materials. Densification provokes a shift of the air entry value (AEV) to higher suction values as it reduces the size and shape of macropores. The initial dry density affects those characteristics, only if suction values are lower than few hundred MPa. Below those suction values, dominant capillary phenomena are controlled by macropores [e.g. 15].

Among others, Lloret et al. [23] studied the volume-change behavior of FEBEX-bentonite in unsaturated conditions. Their experimental program comprised suction-controlled oedometer and constant-volume swelling pressure experiments under different hydro-mechanical paths. Experimental protocols considered the preparation of samples at the hygroscopic water content. Oedometer experiments were conducted on samples, which were characterized by one initial dry density, whereas samples studied in constant-volume swelling pressure experiments were compacted to different initial dry densities. Oedometer experiments indicated that the material rigidified and the yield stress shifted to higher vertical stresses as the suction was increased. The material response considerably depended on the hydro-mechanical path attributable to a

differently evolving microstructure. The imposition of a wetting-loading sequence involves an initial increase in total porosity due to material swelling. Pore-merging accounts for the fact that the mechanical loading affects all pores. A loading-wetting sequence reduces the macro-porosity during mechanical loading and the later collapse of the majority of macropores limits material swelling upon wetting. The former sequence thus yields a greater final total porosity than the latter. There are only a few studies aiming to determine the impact of variations in the initial dry density on the yield behavior of smectite-containing materials upon hydro-mechanical loading. Nowamooz and Masrouri [30] studied the saturated and unsaturated compression behavior of silt/ bentonite-mixtures by means of suction-controlled oedometer experiments. Sample preparation comprised their compaction to different dry densities at the optimum water content. At a given suction, the yield stress increases as the initial dry density increases, and, at a given initial dry density, the material rigidifies as the suction increases. There is still little understanding about whether variations in the initial dry density alter the yield behavior of smectite-containing materials upon hydro-mechanical loading, and how they affect possible hydro-mechanical path dependencies.

Suction-controlled constant-volume swelling pressure experiments of Lloret et al. [23] showed that the evolution of swelling pressure was characterized by a double peak pattern upon stepwise decreasing suctions. The characteristic pattern evolved, regardless of the initial dry density. The first maximum value was attributed to the initial swelling of smectite particles, which was followed by the partial collapse of soil aggregates indicating the yield stress. The second maximum value ensued as the swelling of particles prevails over the collapse of soil aggregates. Romero [33] conducted similar experiments on Boom-clay samples and hypothesized that the yield loci determined in suction-controlled oedometer and constant-volume swell-

ing pressure experiments must coincide. However, only a few studies corroborated the hypothesis [e.g. 4]. Further, there are no information about whether variations in the dry density affect the coincidence.

Experiment results are commonly interpreted and reproduced by adopting the constitutive models proposed in Alonso et al. [2] (*Barcelona Basic Model (BBM)*) and Alonso et al. [3] (*Barcelona Expansive Model (BExM)*). The latter acknowledges the existence of micro- and macropores and is thus capable to reproduce the characteristic features of smectite-containing materials. As respective experimental studies are scarcely available, only a few constitutive models allow to consider the impact of variations in the initial dry density on the hydro-mechanical behavior [38, 43].

In the context of in situ compacted backfill materials, this study aimed to evaluate the impact of variations in the initial dry density on the response of the claystone/ bentonite-mixture to different hydro-mechanical paths. Moreover, it analyzed whether those variations affect the postulated coincidence of yield loci. The evaluation was accomplished by conducting suction-controlled swelling pressure and oedometer experiments on samples which were compacted to different initial dry densities at the optimum water content. Experiments were complemented by analyzing the microstructural and water retention characteristics of the potential backfill material. Obtained results can be useful to improve existing constitutive models regarding the integration of the impact of the initial dry density.

2 Material

Following, the section recapitulated the general characteristics of the mixture studied (e.g. physical characteristics, physico-chemical characteristics, compaction characteristics), and described its microstructural and water retention characteristics afterwards.

2.1 General characteristics

The mixture studied was composed of 70% processed Callovo-Oxfordian (COX) claystone spoil and 30% MX80-bentonite in weight. The latter was limited to 30% in order to reduce mineralogical and physico-chemical incompatibilities between the potential backfill material and the surrounding rock formation. Callovo-Oxfordian claystone spoil arose during the excavation of drifts of Andra URL at a depth of – 490 m (Bure, Meuse/ Haute-Marne region, France). The subsequent processing comprised its crushing and sieving to a maximum grain diameter of 2 mm. The processed material was stored in airtight containers afterwards. Henceforth, processed COX-claystone spoil is referred to as COX_c. At that depth, intact COX-claystone contains 27% carbonates (e.g. calcite, dolomite), 46% phyllosilicates (e.g. smectites, illites), 24% tectosilicates (e.g. quartz, feldspars), and minor fraction of other mineral phases [7]. Likewise, MX80-bentonite (Wyoming, USA) was crushed and sieved to maximum grain diameters of 2 mm and filled into air-tight containers. The dominant mineral phases are phyllosilicates (e.g. smectites), whose fraction is about 84%. The mineralogical composition is completed by tectosilicates (e.g. quartz) [21] .

The mixture was characterized by an initial water content (w_{ini}), liquid limit (LL), plastic limit (PL) and specific gravity (G_s) of 6.4%, 112.5%, 34.7%, and 2.64, respectively [25]. Its cation exchange capacity (CEC) of 39 meq/100g and specific surface area (SSA) of 32 m^2/g were determined by means of the cobalt hexamine method [32] and the BET-method [17], respectively. The cobalt hexamine method also revealed that the exchangeable cation species were dominated by Na^+- and Ca^{2+}-ions. An elevated compaction energy increased the maximum dry density ($\rho_{d,\,max}$) and decreased the optimum water content (w_{opt}) of the mixture [25]. Accordingly, the optimum water content and maximum dry density were 29.0% and 1.45 Mg/m^3, respectively, in the case of standard compaction energy employment, and 18.2% and 1.72 Mg/m^3, respectively, in the case of modified compaction energy employment. The grain

size distribution was determined by means of laser diffractometry and dry sieving and was characterized by 10% - and 60% - passing (D_{10}/ D_{60}) values of 0.008 mm and 0.8 mm, respectively.

2.2 Microstructural characteristics

Mercury intrusion porosimetry (MIP) experiments were conducted on samples initially compacted to dry densities of 1.72 Mg/m³ and 1.44 Mg/m³ at a water content of 18.2% in order to highlight how possible variations in the initial dry density affect the microstructure. The latter value corresponded to a reduction of the initial dry density by about 17.5% with respect to the maximum dry density. Its consideration facilitated to interpret the results of swelling pressure and oedometer experiments presented later. MIP-experiments were conducted by means of an AutoPore IV 9500 (Micromeritics, U.S.A). The MIP-technique bases on the principle of forcing a non-wetting fluid, e.g. mercury, to enter a porous medium by incrementally increasing the injection pressure. A review of the technique is given in Romero and Simms [35]. Prior to the analyzes, samples were dried by heating them up to 80°C under vacuum conditions. Apart from that, the experiment protocol followed that established by Cuisinier and Laloui [8]. Approaches for data processing and presentation were adopted from Juang and Holtz [20].

As depicted in Fig. 2a and Fig. 2c, pore size distribution curves of samples were characterized by two distinct peaks, regardless of the initial dry density. They corresponded to micro- and macropore populations. According to Romero et al. [36], the inflection point of pore size distribution curves indicated the transition from micro- to macropores. Pores, whose diameters were smaller and greater than the diameter at the inflection point, are referred to as micro- and macropores, respectively. Their quantities are expressed by the micro-void ratio (e_m) and macro-void ratio (e_M), respectively. The unaccountable void ratio (e_{un}) is defined as the difference between the calculatable total void ratio (e_{tot}) and the macro-void ratio and accounts for the pores, whose diameter was too small or too large to be detected.

147 The transition of macro- to micropores occurred at pore diameters ranging between 4 and
148 $5x10^2$ nm, regardless of the initial dry density. In all cases, most micropores occurred at a pore
149 diameter of about $2x10^1$ nm. In the case of denser samples, the majority of macropores occurred
150 at a pore diameter of about $8x10^4$ nm. Interestingly, in the case of looser samples, the increasing
151 pore size distribution curve indicated that the diameter, at which the majority of macropores
152 occurred, appeared to exceed the limit of the device. Densification reduced the macro- and
153 unaccountable void ratio by about 50%, whereas the micro-void ratio remained stable. The ob-
154 servation were in accordance with the literature as micropores are expected to react sensitively
155 to the hydraulic but not to the mechanical path, such as those imposed by means of the static
156 compaction method [16, 35, e.g. 36]. The differences in the unaccountable void ratio might be
157 attributed to pores, whose diameters were in the millimeter range involving the low initial dry
158 density.

159 In general, the microstructure of mixture samples comprised micro- and macropores, like
160 other smectite-containing materials. As expected, the latter pore population was significantly
161 reduced by densification. It must be thus assumed that the water retention characteristics of
162 denser and looser material differ considerably.

163 2.3 Water retention characteristics

164 Samples were characterized by initial dry densities of 1.72 Mg/m³ and 1.44 Mg/m³ and a
165 water content of 18.2%. A range between few tens of kPa to some hundreds of MPa were im-
166 posed by combining the osmotic and vapor equilibrium technique. Their individual ranges over-
167 lapped at suctions of about 7 MPa [e.g. 9, 31]. The former technique bases upon the principle
168 that water molecules can go through a semipermeable membrane and move from the pore so-
169 lution to a macro-molecular (polyethylene glycol (PEG)) solution and vice versa. The migration
170 and its direction is driven by a concentration gradient. Suction is functionally related to the
171 concentration of PEG-molecules in solution as their concentration determines the magnitude of

the gradient. A review of the technique is given in Delage and Cui [10]. The vapor equilibrium technique adopts Kelvins equation relating suction to the relative humidity in a closed system. The closed system comprises a gas phase and a liquid phase, whose specific solutes control the relative humidity in the adjacent gas phase. In general, saturated salt solutions are employed as a liquid phase. A review of the technique is given in Delage et al. [12] and Delage et al. [13].

As depicted in Fig. 3, denser samples were initially characterized by lower void ratios and higher degrees of saturation due to the higher initial dry density. Upon hydration, the void ratio and degree of saturation of looser and denser samples increased comparably. Drying had no considerable consequences on both sample types with regard to their void ratios. It affected the degree of saturation of denser samples more significantly than that of looser samples.

The impact of variations in the initial dry density appeared to vanish when imposed suction exceeded values of 200 MPa. This observation was in accordance with the results of microstructural analysis as the vanishing impact of initial dry density indicated the existence of micro- and macropores (Fig. 2). The imposition of a suction higher than 200 MPa involved the fact that residual water was available only in micropores, whose size and shape were insensitive to compaction and varying initial dry densities. According to the different diffuse double layer theories, electrostatic interactions between the water molecules and the clay mineral surfaces account for a complete immobilization of the residual water in micropores [e.g 34].

In general, the water retention characteristics of differently dense mixture samples confirmed the results of microstructural analysis as the vanishing impact of initial dry density at high suctions indicated the existence of micro-and macropores.

3 Oedometer and constant-volume swelling pressure experiments

The unsaturated compression and swelling behavior were studied by conducting oedometer and constant-volume swelling pressure experiments, in which the suction was controlled by means of the osmotic technique. Further, different hydro-mechanical paths were imposed to

197 analyze the impact of variations in the dry density on possible path dependencies. The experi-
198 ment approach considering variations in the initial dry density, the sample preparation, the ex-
199 periment protocols, and the experiment program are described below.

200 3.1 Approach

201 Full-scale experiments conducted in situ (e.g. the "Backfill and Plug Test" [18], the "Pro-
202 totype repository" [6]) highlighted the issues involving the employment of conventional com-
203 paction techniques to install smectite-containing backfill materials in situ. Their experiment
204 protocols envisaged compacting backfill materials to the maximum dry density at the optimum
205 water content in a layer-wise manner. Highest swelling pressure and lowest compressibility
206 were expected to be reached by this means [e.g. 26]. Unlike the initial water content, whose
207 value remained stable in the cross section of the drift, the initial dry density decreased by up to
208 20% with respect to the maximum dry density. They attributed this finding to a loss of compac-
209 tion energy ensuing as the handling of the compactor became difficult, in particular close to the
210 drift top and drift walls.

211 In order to portray spatial variations in the initial dry density, samples were compacted to
212 the maximum dry density of 1.72 Mg/m³ at the optimum water content of 18.2%, which was
213 obtained by means of modified Proctor experiments. They were complemented by samples
214 characterized by dry densities of 1.66 Mg/m³, 1.59 Mg/m³, and 1.44 Mg/m³ and a water con-
215 tent of 18.2%. The values corresponded to a reduction of the dry density by 2.5%, 7.5% and
216 17.5%, respectively, with respect to the maximum dry density.

217 3.2 Sample preparation

218 The material was prepared at the optimum water content and then filled in an airtight
219 container. Deaired/ demineralized water was added in order to reach the optimum water content
220 [25]. Samples were compacted to the different dry densities at the optimum water content by
221 means of the static compaction method at a controlled deformation rate of 0.1 mm/s. Samples,

whose microstructural and water retention characteristics were previously presented, were similarly prepared. Henceforth, the type indicates the initial dry density of samples. Their initial characteristics are compiled in Table 1.

3.3 Suction-controlled oedometer experiments

The protocol of suction-controlled oedometer experiments considered samples of all types. The cell employed in suction-controlled oedometer experiments was composed of a piston, mold, and base (e.g. Delage et al. [11] or Nowamooz and Masrouri [29] for further information about its design). The base was characterized by one inlet, one outlet and a mesh, so solutions could be circulated beneath the mesh. It covered a groove spiraling to the center axis of the cylindrical cell and connecting the inlet and outlet. In combination with a semi-permeable membrane separating the sample from the mesh, the design allowed to adopt the osmotic technique in order to impose suctions. The oedometer allowed to apply vertical stresses of up to 3000 kPa. PEG-reservoirs were placed in temperature-controlled baths in order to minimize temperature effects.

3.4 Suction-controlled constant-volume swelling pressure experiments

Samples of all types were considered in order to study the evolution of swelling pressure upon stepwise hydration. The constant-volume swelling pressure cell proposed by Yigsaw et al. [40] was similarly designed allowing to adopt the osmotic technique. However, a porous disc was employed instead of the mesh, and the piston was substituted for a lid, which contained the load sensor. By eventually screwing the components together, a pre-stress of 50 kPa was imposed.

3.5 Hydro-mechanical paths and experimental program

The protocol of suction-controlled swelling pressure and oedometer experiments comprised different hydro-mechanical paths depicted in Fig. 4 and Fig. 5, respectively. Their imposition aimed to determine how different paths affect the swelling and compression behavior of

247 the potential backfill material, in particular in unsaturated conditions. Since backfill materials
248 are not expected to undergo drying, hydration referred exclusively to the (stepwise) saturation
249 of the mixture, whose initial suction was about 2700 kPa (Table 1).

250 Hydro-mechanical paths A, B, C, and D differed in the magnitude of the initial hydration
251 step followed by stepwise mechanical loading and unloading. Hydro-mechanical loads were
252 changed when strains stabilized at rates lower than 0.5 % (of the initial sample height) per day.

253 Hydro-mechanical paths E, F, and G differed in the number of stages, in which different
254 suctions were imposed. Imposed suctions were decreased when the swelling pressure stabilized
255 at rates lower than 5 kPa per day.

256 Henceforth, samples are identifiable by means of their sample type and imposed hydro-
257 mechanical paths. The prefix refers to the sample type, whereas the imposed hydro-mechanical
258 path is indicated by the suffix. For instance, sample I - D was characterized by an initial dry
259 density of 1.72 Mg m^{-3}, whose compression behavior was analyzed by adopting hydro-mechan-
260 ical path D (Fig. 4). The experiment program developed is described in Table 2.

261 It was believed that this comprehensive experimental program allowed to evaluate how
262 variations in the initial dry density affect the behavior of a potential backfill material under
263 different hydro-mechanical paths.

264 4 Results

265 Following, the results of suction-controlled oedometer and constant-volume swelling
266 pressure experiments are presented. Since the free-swell potential experiments represented the
267 first stage of oedometer experiments, their results are described in the corresponding section.

268 4.1 Suction-controlled oedometer experiments

269 Oedometer experiments were conducted on type I- to type IV-samples by imposing hy-
270 dro-mechanical paths A to D. They were aimed at studying how the one-dimensional compres-
271 sion behavior of the mixture varies as response to the different initial dry densities of samples

and imposed hydro-mechanical paths. Additionally, information about the free-swell potential were provided. Their results are depicted in Fig. 6a to Fig. 6h. For clarification purpose, the presentation of the results obtained while unloading is omitted.

Compression curves were characterized by two or three zones, in which the slope of the compression line changed. Hydro-mechanical paths C and D involved two zones, whereas the imposition of hydro-mechanical paths A and B implied the development of three zones constituting s-shaped compression curves. Compression lines converged as net vertical stresses were increased beyond about 1000 kPa. Those characteristics were observed, regardless of the initial dry density of samples. The intersection of compression curves of less dense samples cannot be reasonably explained, yet (compare Fig. 6h). In elastoplastic frameworks [e.g. 2], the first and second zones are referred to as the elastic and plastic domains, which are separated by the yield stress. Deformations in the elastic domain appeared to be little affected by varying initial dry densities, whereas decreasing suctions involved greater elastic deformations. Deformations in the plastic domain became less pronounced as initial dry densities and imposed suctions increased. In addition, similarly dense samples exhibited smaller plastic deformations in response to increasing suctions. Among the different sample types, yield stresses appeared to converge as initially imposed suctions were reduced.

Oedometer experiments also indicated that the free-swell potential increased as the initial dry density was increased, in particular upon imposing lower initial suctions.

In general, the initial dry density affected the one-dimensional compression behavior of mixture samples more considerably when higher suctions were imposed. In saturated state, compression curves appeared to be comparable with regard to their characteristics and shape. The free-swell potential was considerably affected by the initial dry density, in particular in ranges of lower suctions.

4.2 Suction-controlled constant-volume swelling pressure experiments

Constant-volume swelling pressure cells controlling suction by means of the osmotic technique were employed in order to study the swelling pressure evolution of the mixture under different hydro-mechanical paths. Evolution of swelling pressure recorded are depicted in Fig. 7a and Fig. 7b.

In the case of sample II-E, the evolution was not measured due to a malfunction of the load sensor. It still became evident in Fig. 7a that the stabilized swelling pressure at each suction stage increased as the initial dry density increased. The pattern of the curves was generally characterized by a post-peak stabilization at lower or comparable stresses. In the cases of type III- and IV-samples, the decrease of swelling pressure occurred upon imposing a suction smaller than 1000 kPa, whereas, in the case of the type I-sample, there was only a slight reduction and ensued when suctions were smaller than 100 kPa. As highlighted in Fig. 7b, the mixture reacted to the imposition of different hydration paths identically, since the stabilized swelling pressures at the corresponding suction stages differed negligibly.

In general, suction-controlled constant-volume swelling pressure experiments revealed that the unsaturated swelling pressure of the mixture depended on the initial dry density rather than on the hydraulic path. Further, the results depicted in Fig. 7b indicated a good repeatability of swelling pressure experiments.

5 Discussion

The discussion adopted the elastoplastic frameworks proposed in Alonso et al. [2] and Alonso et al. [3]. It analyzed how variations in the initial dry density affect the compression and swelling behavior of mixture samples. The first and second sections are followed by a comparison which evaluated how those variations alter the response of materials to the different hydro-mechanical paths, in particular the yield behavior. Although representing the first stage of the suction-controlled oedometer experiments, it appears to be more suitable to discuss the results

of free-swell potential experiments in conjunction with those of the swelling pressure experiments.

5.1 Compression behavior

Suction-controlled oedometer experiments indicated that the shape of compression curves depended on the hydro-mechanical path, in particular on the initially imposed wetting. The dependency was observed, regardless of the initial dry density. The imposition of hydro-mechanical paths C and D led to compression curves characterized by the elastic and plastic domain. In contrast, s-shaped compression curves ensued through the imposition of hydro-mechanical paths A and B. Their nonlinear compression behavior in the plastic domain disagreed with the formulation of the virgin compression line, whose slope is described by the parameter $\lambda(s)$ [2]. The applicability of the framework thus appeared to be limited.

In general, at a given suction, loading induces the collapse of macropores, and in turn, increases the degree of saturation. In other words, unsaturated samples could saturate through compaction [e.g. 28]. The nonlinear behavior might be related to the fact that the compressibility varied as the degree of saturation increased [e.g. 44]. Models proposed in Gallipoli et al. [14] and Zhou et al. [44] relate the compressibility to the degree of saturation, instead of suction. By this means, they allow to describe the transition of the compressibility in unsaturated state to that in saturated state through compaction. This prediction was consistent as compression curves converged at high vertical stresses ($\sigma_v \geq 1000$ kPa), regardless of the imposed suction. In the context of in situ compacted backfill materials, the prediction implied a negligible impact of the saturation state on the compression behavior when the overburden pressure fully affects the backfill material.

In the frameworks proposed in Alonso et al. [2] and Alonso et al. [3], the loading-collapse (LC) curve gives the functional relation between the yield stress and imposed suction. Corresponding yield loci were derived from suction-controlled oedometer experiments. As depicted

346 in Fig. 8a, the variation of yield stress with imposed suction was almost identical, in the cases
347 of type I-, II-, and III-samples. LC-curves thus coincided. Yield stresses of type IV-samples
348 were lower, in particular when hydro-mechanical paths C (s = 200 kPa) and D (s = 2000 kPa)
349 were imposed. In ranges of lower suctions, the two LC-curves converged. Two conclusions can
350 be drawn from Fig. 8. At higher suctions, slight variations in the initial dry density had no
351 impact on the yield behavior. There was an apparent threshold, below which the initial dry
352 density came into effect. At lower suctions, the impact of variations in the initial dry density
353 vanished. It was manifested by the convergence of LC-curves.

354 At lower suctions, crystalline swelling and partial particle breakup ensued as the hydra-
355 tion front propagated entirely through the sample under free conditions. Collapse of macropores
356 was less probable due to the small vertical stress ($\sigma_v \approx 10$ kPa). The processes involved an
357 increase in micropores and a decrease in macropores as swelling particles penetrated the macro-
358 pores. Not only did pore merging turn the bimodal pore size distribution function into a uni-
359 modal one, it also increased the total porosity, regardless of the initial dry density [e.g. 41, 42].
360 In general, a unimodal pore size distribution function implies that mechanical loading affects
361 the overall structure. At lower suctions, loading in the elastic domain adapted the amount of
362 pores in all samples, as indicated by the coinciding void ratios in Fig. 8b. The pores collapsed
363 under comparable stresses, thus the stiffness of the overall structure and in turn, the yield
364 stresses appeared to converge.

365 In contrast, at higher suctions, the structure of mixture samples was characterized by mi-
366 cro- and macropores, and mechanical loading affected only the aggregates surrounding the lat-
367 ter pore population. LC-curves of type I-, II-, and III-samples might coincide due to a still com-
368 parable amount of macropores and, in turn, a similar stiffness of soil aggregates. Accordingly,
369 the elevated macroporosity in type IV-samples accounted for the lower yield stresses. It might

be of interest to corroborate the hypothesis of comparable structures after free swelling by means of microstructural investigations (e.g. MIP-experiments).

In the context of in situ compacted backfill materials, the results of suction-controlled oedometer experiments highlighted that the initial dry density has an impact of the compression behavior of the mixture, in particular on the yield behavior, only if lower vertical stresses and higher suctions are imposed. If samples saturate under free-swell conditions, an adaption of the total porosity appears to involve a comparable stiffness of the overall structure.

5.2 Swelling behavior

Suction-controlled constant-volume swelling pressure experiments indicated that the evolution of swelling pressure was characterized by a post-peak stabilization at lower or comparable stresses. Although the increase in initial dry density accompanied an increase in swelling pressure at a given suction (Fig. 7a), there was no functional relation between initial dry density and swelling pressure.

As implied in the introduction, Lloret et al. [23] adopted parts of the elastoplastic framework proposed in Alonso et al. [3] in order to interpret the double peak pattern. The initial reduction of suction caused homogeneous swelling of particles. Increasing vertical stresses compensated for the swelling of particles as the stiffness of soil aggregates was high. Decreasing vertical stresses followed the first maximum value and indicated that the yield stress was reached. The partial collapse of macropores lowered the stiffness of soil aggregates and progressing swelling of particles cannot compensate for the collapse of macropores. As the reduction of suction reduction, swelling of particles prevailed over collapse of macropores, and increasing vertical stresses compensated for the swelling of particles again. The phenomenological interpretations proposed in Massat et al. [24] and Yigsaw et al. [40] were similar to that of Lloret et al. [23]. Yet, they specified that macrostructural rearrangements accounted for an increase in material stiffness and a consequent dominance of swelling of particles. In this study,

the evolution of swelling pressure was characterized by a post-peak stabilization at lower or comparable stresses. In the cases of type I-samples, vertical stresses stabilized at comparable values after reaching the peak. Their lower initial macroporosity apparently limited the structural rearrangement, in particular the collapse of macropores. Conversely, in the cases of type III- and IV-samples, the swelling of particles appeared to be less pronounced than the collapse of macropores, thus the vertical stresses stabilized at lower stresses.

Wang et al. [39] described a potential functional relation between the imposed suction and swelling pressure which implied a monotonous increase in swelling pressure. Since they attributed this finding to the homogeneous swelling of particles and the high stability of soil aggregates, the question was raised why aggregates might be differently stable.

Middelhoff et al. [25] conducted constant-volume swelling pressure experiments on mixture samples prepared to the same initial conditions. Their experiment protocol comprised the direct saturation of samples with deaired/ deionized water. The results complemented those recently obtained and highlighted the hydraulic path independency of the material, as depicted in Fig. 9a and Fig. 9b. The independence appeared to be valid, regardless of the initial dry density of the material. Wang et al. [39] conducted similar swelling pressure experiments on compacted bentonite/ claystone-mixture samples, whose mineralogical composition was dominated by smectites. They also reported on a hydraulic path independency. According to their interpretation, the direct and stepwise saturation triggered sequentially comparable structural rearrangements and led eventually to a similar microstructure.

The protocol of suction-controlled oedometer experiments comprised the determination of the free-swell potential of mixture samples at their initial stage. The relationship between the initial dry density and free-swell potential of samples can be described by a linear function, whose slope increased logarithmically as the suction decreases. In the case of suctions being equal to 2000 kPa, no swelling was observed. Presumably, the increasing smectite mass in

denser samples caused the linear relation since each particle can undergo crystalline swelling and particle breakup under the availability of water molecules [e.g. 22]. Major macrostructural rearrangements were less probable due to the low initial vertical load.

In general, suction-controlled constant-volume swelling pressure experiments indicated that stepwise wetting involved a non-monotonic increase in swelling pressure, regardless of the initial dry density. The post-peak stabilization at lower or comparable stresses was attributed to structural rearrangements, in particular particle swelling and partial macropore collapse. In the case of denser samples, the latter aspect might account for the stabilization at comparable stresses. Accordingly, the partial collapse was less significant due to the smaller amount of macropores therein. The evolution of swelling pressure was hydraulic path independent potentially attributable to a similar final microstructure. The free-swell potential experiments indicated a functional relation between the initial dry density and final free-swell potential at a given suction. It was attributed to the availability of water molecules and the larger amount of smectite particles in denser samples.

5.3 Comparison of yield behavior

As described above, the (suction-controlled) propagation of the hydration front through the sample under constant-volume conditions involved the initial swelling of particles, followed by the collapse of aggregates and the final dominance of particle swelling over aggregate collapse. The swelling pressure evolved in conjunction with those structural rearrangements. In contrast, under oedometric conditions, structural rearrangements were terminated before loading. The differently rearranging structure might account for the fact that the yield loci of denser samples differed significantly, whereas those of looser samples coincided, as depicted in Fig. 10.

In the case of type I- and III-samples, the partial collapse of aggregates and the subsequent swelling of particles appeared to increase the density of the material and, in turn, the stiffness

of the overall structure [24]. Their yield stress increased as a consequence. Type IV-samples were characterized by an elevated fraction of macropores, and their partial collapse cannot be compensated by the swelling of particles. The densification was less effective, and the stiffness of the overall structure measured under constant-volume conditions became comparable to that determined under oedometric conditions. Indeed, the findings partially corroborated the hypothesis suggested by Romero [33] as the yield loci of looser samples coincided. However, the yield behavior of denser samples appeared to considerably depend on the hydro-mechanical path. Conclusion

The French reference considers a mixture composed of 70% processed Callovo-Oxfordian claystone spoil and 30% MX80-bentonite to be a material, which could be potentially employed to backfill drifts and shafts of the future repository for intermediate- and high-level radioactive waste in the clay-rich Callovo-Oxfordian sedimentary rock formation. Regardless of the saturation state, the convergence of the surrounding rock formation likely induces mechanical loading. Thus, the occurrence of different hydro-mechanical paths is possible. Installed by means of conventional compaction methods, the backfill material is likely characterized by spatial variations in its initial dry density. Since the initial dry density is one of the factors controlling the water retention characteristics and hydro-mechanical behavior of smectite-containing material, it is of major relevance to analyze the impact of its variations on the performance of claystone/ bentonite-mixtures, in particular in unsaturated state.

At its initial stage, this laboratory experimental program analyzed the mixture with regard to its microstructural and water retention characteristics. Subsequent suction-controlled oedometer and constant-volume swelling pressure experiments aimed to evaluate how variations in the initial dry density affect the compression and swelling behavior. The final comparison of experiment results revealed whether the hydro-mechanical behavior of the mixture depends on

the hydro-mechanical path, and whether variations in the dry density have an impact on possible dependencies. Following conclusions can be drawn from the experiments conducted:

1. The results of microstructural analysis agreed with the trends generally described in the literature. In contrast to micropores, whose amount remained stable, macropores were considerably affected by densification. A reduction of dry density by about 20% decreased their amount by about 50%.
2. As expected, water retention characteristics highlighted the existence of micro- and macropores since the impact of the initial dry density vanished at higher suctions. The observation was related to the fact that micropores control capillary phenomena at higher suctions.
3. The impact of the initial dry density on the compression behavior of mixture samples vanished when higher vertical stresses or lower suctions were imposed. Although suctions were imposed, the compression curves of unsaturated samples converged into those of saturated samples at higher stresses.
4. At a given suction, the free-swell potential of the mixture was linearly related to the initial dry density. In turn, the slope of this linear function varied logarithmically with the imposed suction. The findings were attributed to the larger amount of smectite particles in denser samples and to the greater availability of water molecules at lower suctions.
5. Suction-controlled hydration of mixture samples under constant-volume conditions involved the evolution of swelling pressure, whose development was characterized by a post-peak stabilization at lower or comparable stresses. The pattern evolved regardless of the initial dry density and was attributed to rearrangements at the micro- and macrostructural level. The swelling pressure increased with increasing initial dry density at a given suction. Apart from those findings, experiments revealed that the evolution of swelling

pressure was independent of the hydraulic path potentially attributable to a similar final microstructure.

6. The comparison of results highlighted that the initial dry density of samples had an impact on their hydro-mechanical path dependency. In the case of looser samples, the yield behavior under constant-volume and oedometric conditions was comparable, whereas, in the case of denser samples, the yield stresses were shifted to lower values under oedometric conditions. The difference in yield locus position was attributed to an adaption of the total porosity and a comparable stiffness of the overall structure.

This study confirmed that the microstructural and water retention characteristics of the claystone/ bentonite-mixture considerably changed as a response to variations in their initial dry density. Variations in the initial dry density had a significant impact on the swelling behavior of the mixture, regardless of the saturation state. Regarding the compression behavior, the impact vanished as lower suctions or higher vertical stresses were imposed. In the context of in situ compacted backfill materials, neither the initial dry density nor the saturation state accordingly have an impact on the compression behavior when the material is subjected to the overburden pressure once the concrete lining degrades. The evolution of swelling pressure under constant-volume conditions was hydraulic path independent, whereas the yield behavior was hydro-mechanical path independent only when the initial dry density of the material was lower. Regarding future laboratory experimental studies, it might be of interest to corroborate the hypothesis of the comparable stiffness of the overall structure by complementing the different stages in oedometer experiments by means of X-ray tomography.

Funding

The work presented in this paper has been carried out during the preparation of the PhD thesis of the first author, which is funded by Andra (France), the French agency in charge of the management and disposal of nuclear waste.

Conflicts of interest

The authors wish to confirm that there are no known conflicts of interest associated with this publication and there has been no significant financial support for this work that could have influenced its outcome.

Availability of data and material

The datasets generated during and/or analysed during the current study are available from the corresponding author on reasonable request.

Author's contributions

Conceptualization: Marvin Middelhoff, Olivier Cuisinier, Farimah Masrouri, Jean Talandier; **Methodology:** Marvin Middelhoff, Olivier Cuisinier, Farimah Masrouri, Jean Talandier; **Formal analysis and investigations:** Marvin Middelhoff; **Writing – original draft preparation:** Marvin Middelhoff; **Writing – review and editing:** Marvin Middelhoff, Olivier Cuisinier, Farimah Masrouri, Jean Talandier; **Funding acquisition:** Olivier Cuisinier, Farimah Masrouri, Jean Talandier; **Resources:** Jean Talandier; **Supervision:** Olivier Cuisinier, Farimah Masrouri, Jean Talandier

References

1. Alonso EE, Gens A, Whight D (1987) General report. In: Hanrahan ET, Orr TLL, Widdis TF (eds) Groundwater Effects in Geotechnical Engineering. A. A. Balkema, Rotterdam, Brookfield, pp 1087–1146
2. Alonso EE, Gens A, Josa A (1990) A constitutive model for partially saturated soils. Géotechnique 40:405–430. doi: 10.1680/geot.1990.40.3.405
3. Alonso EE, Vaunat J, Gens A (1999) Modelling the mechanical behaviour of expansive clays. Engineering Geology 54:173–183. doi: 10.1016/S0013-7952(99)00079-4
4. Alonso EE, Romero E, Hoffmann C et al. (2005) Expansive bentonite–sand mixtures in cyclic controlled-suction drying and wetting. Engineering Geology 81:213–226. doi: 10.1016/j.enggeo.2005.06.009
5. ANDRA (2005) Dossier 2005 Argile Synthesis. Evaluation of the feasibility of a geological repository in an argillaceeous formation. Meuse/ Haute-Marne site. Collection les Rapports, vol 268. ANDRA, Châtenay-Malabry
6. Börgesson L, Gunnarsson D, Johannesson L-E et al. (2002) Äspö Hard Rock Laboratory. Prototype Repository - Installation of buffer, canisters, backfill and instruments in section 1. Technical Report, Stockholm
7. Conil N, Talandier J, Djizanne H et al. (2018) How rock samples can be representative of in situ condition: A case study of Callovo-Oxfordian claystones. Journal of Rock Mechanics and Geotechnical Engineering 10:613–623. doi: 10.1016/j.jrmge.2018.02.004
8. Cuisinier O, Laloui L (2004) Fabric evolution during hydromechanical loading of a compacted silt. Int J Numer Anal Meth Geomech 28:483–499. doi: 10.1002/nag.348
9. Cuisinier O, Masrouri F (2005) Hydromechanical behaviour of a compacted swelling soil over a wide suction range. Engineering Geology 81:204–212. doi: 10.1016/j.enggeo.2005.06.008

10. Delage P, Cui YJ (2008) An evaluation of the osmotic method of controlling suction. Geomechanics and Geoengineering 3:1–11. doi: 10.1080/17486020701868379
11. Delage P, Vicol T, Suraj de Silva, G. P. R. (1992) Suction controlled testing of non-saturated soils with an osmotic consolidometer. In: The proceedings of the 7th interna-tional conference on expansive soils. Texas Tech Universtiy Press, Lubbock, pp 206–211
12. Delage P, Howat M, Cui Y (1998) The relationship between suction and swelling properties in a heavily compacted unsaturated clay. Engineering Geology 50:31–48. doi: 10.1016/S0013-7952(97)00083-5
13. Delage P, Romero E, Tarantino A (2008) Recent developments in the techniques of controlling and measuring suction in unsaturated soils. In: Toll DG, Augarde CE (eds) Unsaturated soils: Advances in Geo-Engineering. Proceedings of the 1st European Conference on Unsaturated Soils (E-UNSAT 2008, Durham, United Kingdom, 02/07/2008 - 04/07/2008). CRC Press/Balkema, Boca Raton, Fla., pp 33–52
14. Gallipoli D, Gens A, Sharma R et al. (2003) An elasto-plastic model for unsaturated soil incorporating the effects of suction and degree of saturation on mechanical behavior. Géotechnique 53:123–135. doi: 10.1680/geot.2003.53.1.123
15. Gao Y, Sun DA (2017) Soil-water retention behavior of compacted soil with different densities over a wide suction range and its prediction. Computers and Geotechnics 91:17–26. doi: 10.1016/j.compgeo.2017.06.016
16. Gao Y, Sun DA, Zhu Z et al. (2019) Hydromechanical behavior of unsaturated soil with different initial densities over a wide suction range. Acta Geotech 14:417–428. doi: 10.1007/s11440-018-0662-5
17. Gregg SJ, Sing KSW (1969) Adsorption, surface area and porosity, Second printing. Academic Press, London

19. Hoffmann C, Alonso EE, Romero E (2007) Hydro-mechanical behaviour of bentonite pellet mixtures. Physics and Chemistry of the Earth, Parts A/B/C 32:832–849. doi: 10.1016/j.pce.2006.04.037
20. Juang CH, Holtz RD (1986) A probabilistic permeability model and the pore size density function. Int J Numer Anal Meth Geomech 10:543–553. doi: 10.1002/nag.1610100506
22. Likos WJ, Wayllace A (2010) Porosity evolution of free and confined bentonites during interlayer hydration. Clays Clay Miner 58:399–414. doi: 10.1346/CCMN.2010.0580310
23. Lloret A, Villar MV, Sánchez M et al. (2003) Mechanical behaviour of heavily compacted bentonite under high suction changes. Géotechnique 53:27–40. doi: 10.1680/geot.2003.53.1.27
24. Massat L, Cuisinier O, Bihannic I et al. (2016) Swelling pressure development and inter-aggregate porosity evolution upon hydration of a compacted swelling clay. Applied Clay Science 124-125:197–210. doi: 10.1016/j.clay.2016.01.002
25. Middelhoff M, Cuisinier O, Masrouri F et al. (2020) Combined impact of selected material properties and environmental conditions on the swelling pressure of compacted claystone/bentonite mixtures. Applied Clay Science 184:105389. doi: 10.1016/j.clay.2019.105389
26. Mitchell JK, Soga K (2005) Fundamentals of soil behavior, 3rd edition. John Wiley & Sons, Hoboken, N.J.
27. Monroy R, Zdravkovic L, Ridley A (2010) Evolution of microstructure in compacted London Clay during wetting and loading. Géotechnique 60:105–119. doi: 10.1680/geot.8.P.125
28. Nagaraj TS, Murthy BRS, Vatsala A et al. (1990) Analysis of Compressibility of Sensitive Soils. Journal of Geotechnical Engineering 116:105–118. doi: 10.1061/(ASCE)0733-9410(1990)116:1(105)

29. Nowamooz H, Masrouri F (2008) Hydromechanical behaviour of an expansive bentonite/silt mixture in cyclic suction-controlled drying and wetting tests. Engineering Geology 101:154–164. doi: 10.1016/j.enggeo.2008.04.011
30. Nowamooz H, Masrouri F (2009) Density-dependent hydromechanical behaviour of a compacted expansive soil. Engineering Geology 106:105–115. doi: 10.1016/j.enggeo.2009.03.010
31. Nowamooz H, Masrouri F (2010) Relationships between soil fabric and suction cycles in compacted swelling soils. Engineering Geology 114:444–455. doi: 10.1016/j.enggeo.2010.06.005
32. Orsini L, Remy JC (1976) Utilisation du chlorure de cobaltihexammine pour la détermination simultanée de la capacité d'échange et des bases échangeables des sols. Bulletin de l'AFES Science du Sol 4:269–275
33. Romero E (1999) Characterisation and thermo-hydro-mechanical behaviour of unsaturated boom clay. An experimental study. PhD-Thesis, Universitat Politècnica de Catalunya
34. Romero E (2013) A microstructural insight into compacted clayey soils and their hydraulic properties. Engineering Geology 165:3–19. doi: 10.1016/j.enggeo.2013.05.024
35. Romero E, Simms PH (2008) Microstructure Investigation in Unsaturated Soils: A Review with Special Attention to Contribution of Mercury Intrusion Porosimetry and Environmental Scanning Electron Microscopy. Geotech Geol Eng 26:705–727. doi: 10.1007/s10706-008-9204-5
36. Romero E, Gens A, Lloret A (1999) Water permeability, water retention and microstructure of unsaturated compacted Boom clay. Engineering Geology 54:117–127. doi: 10.1016/S0013-7952(99)00067-8

37. Sivakumar V, Tan WC, Murray EJ et al. (2006) Wetting, drying and compression characteristics of compacted clay. Géotechnique 56:57–62. doi: 10.1680/geot.2006.56.1.57
38. Sun DA, Sheng DC, Cui HB et al. (2007) A density-dependent elastoplastic hydro-mechanical model for unsaturated compacted soils. Int J Numer Anal Meth Geomech 31:1257–1279. doi: 10.1002/nag.579
39. Wang Q, Tang AM, Cui Y-J et al. (2012) Experimental study on the swelling behaviour of bentonite/claystone mixture. Engineering Geology 124:59–66. doi: 10.1016/j.enggeo.2011.10.003
40. Yigzaw ZG, Cuisinier O, Massat L et al. (2016) Role of different suction components on swelling behavior of compacted bentonites. Applied Clay Science 120:81–90. doi: 10.1016/j.clay.2015.11.022
41. Yuan S, Liu X, Sloan SW et al. (2016) Multi-scale characterization of swelling behaviour of compacted Maryland clay. Acta Geotech 11:789–804. doi: 10.1007/s11440-016-0457-5
42. Yuan S, Buzzi O, Liu X et al. (2019) Swelling behaviour of compacted Maryland clay under different boundary conditions. Géotechnique 69:514–525. doi: 10.1680/jgeot.17.P.140
43. Zhou A-N, Sheng DC (2015) An advanced hydro-mechanical constitutive model for unsaturated soils with different initial densities. Computers and Geotechnics 63:46–66. doi: 10.1016/j.compgeo.2014.07.017
44. Zhou A-N, Sheng D, Sloan SW et al. (2012) Interpretation of unsaturated soil behaviour in the stress–saturation space. Computers and Geotechnics 43:111–123. doi: 10.1016/j.compgeo.2012.02.009

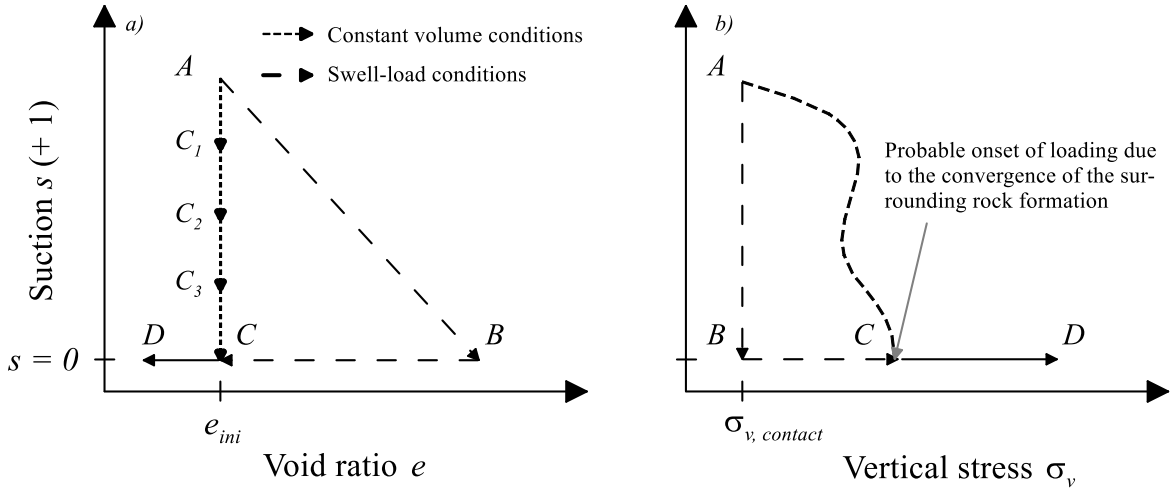

658

659 **Fig. 1** Possible combinations of hydraulic and mechanical paths subjected to the backfill upon terminat-
660 ing the installation phase

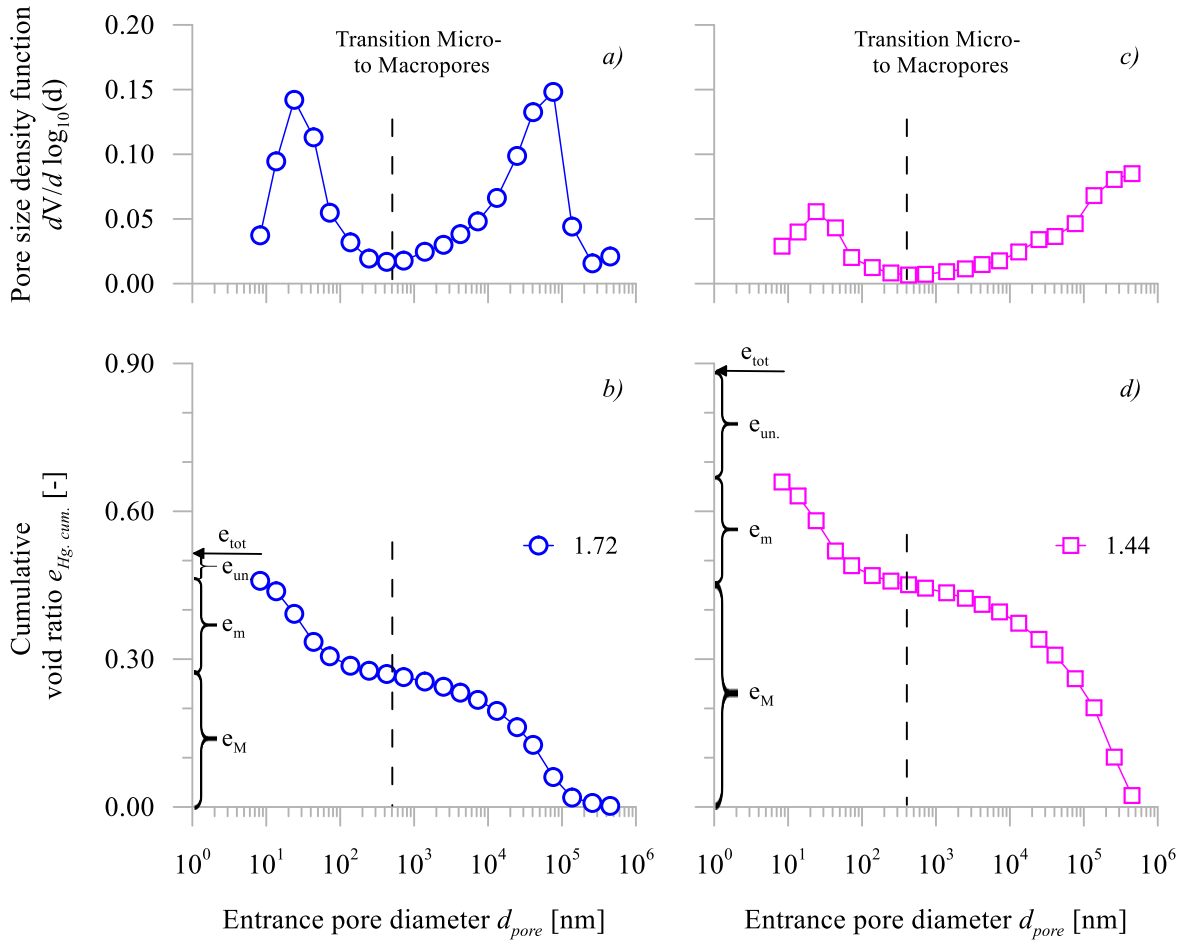

661

662 **Fig. 2** Results of mercury intrusion porosimetry (MIP) experiments conducted on samples characterized
663 by initial dry densities of $\rho_{d,ini}$ = 1.72 Mg/m³ and $\rho_{d,ini}$ = 1.44 Mg/m³

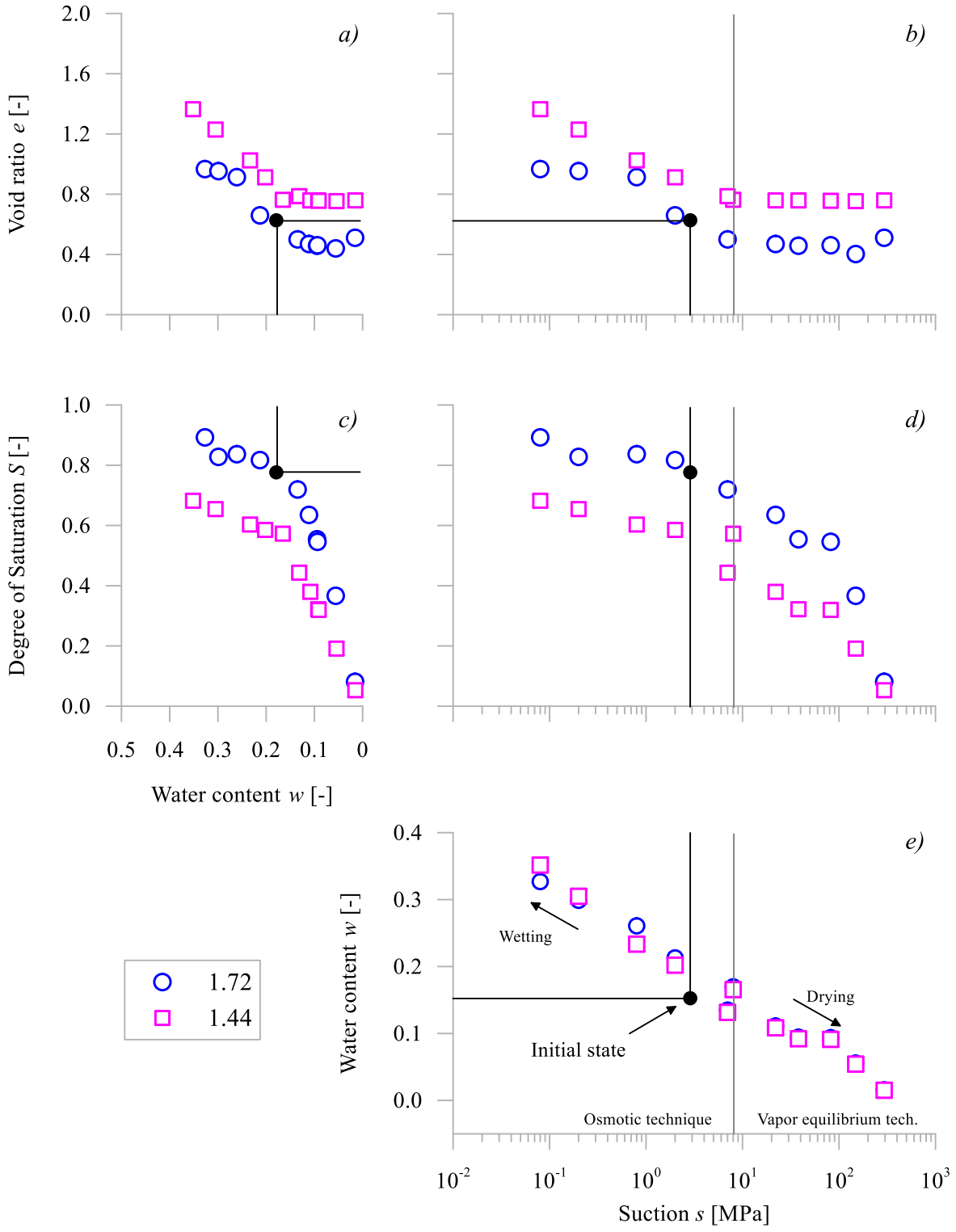

Fig. 3 Water retention characteristics of mixture samples characterized by initial dry densities of $\rho_{d,ini}$ = 1.72 Mg/m³ and $\rho_{d,ini}$ = 1.44 Mg/m³

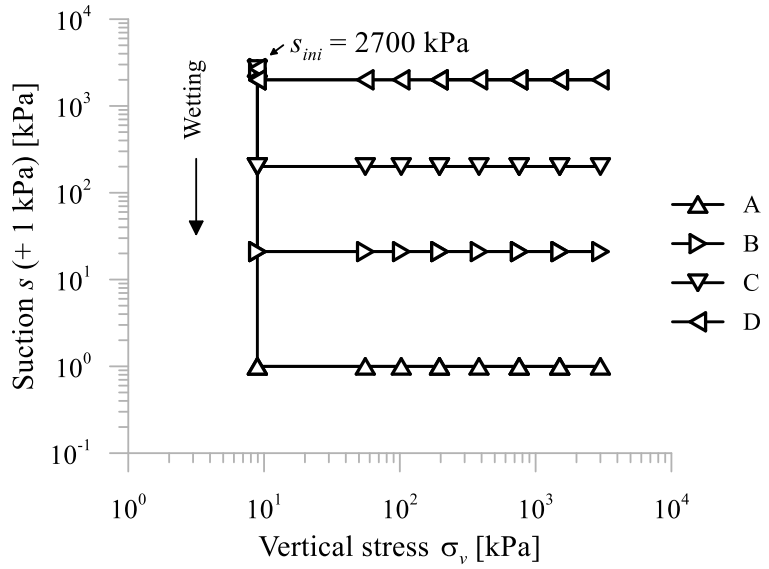

667

668 **Fig. 4** Hydro-mechanical paths followed in suction-controlled oedometer experiments

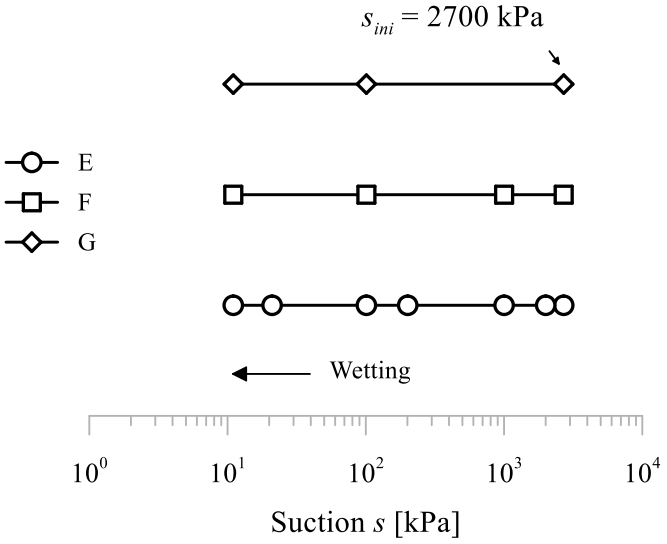

669

670 **Fig. 5** Hydration paths followed in suction-controlled constant-volume swelling pressure experiments

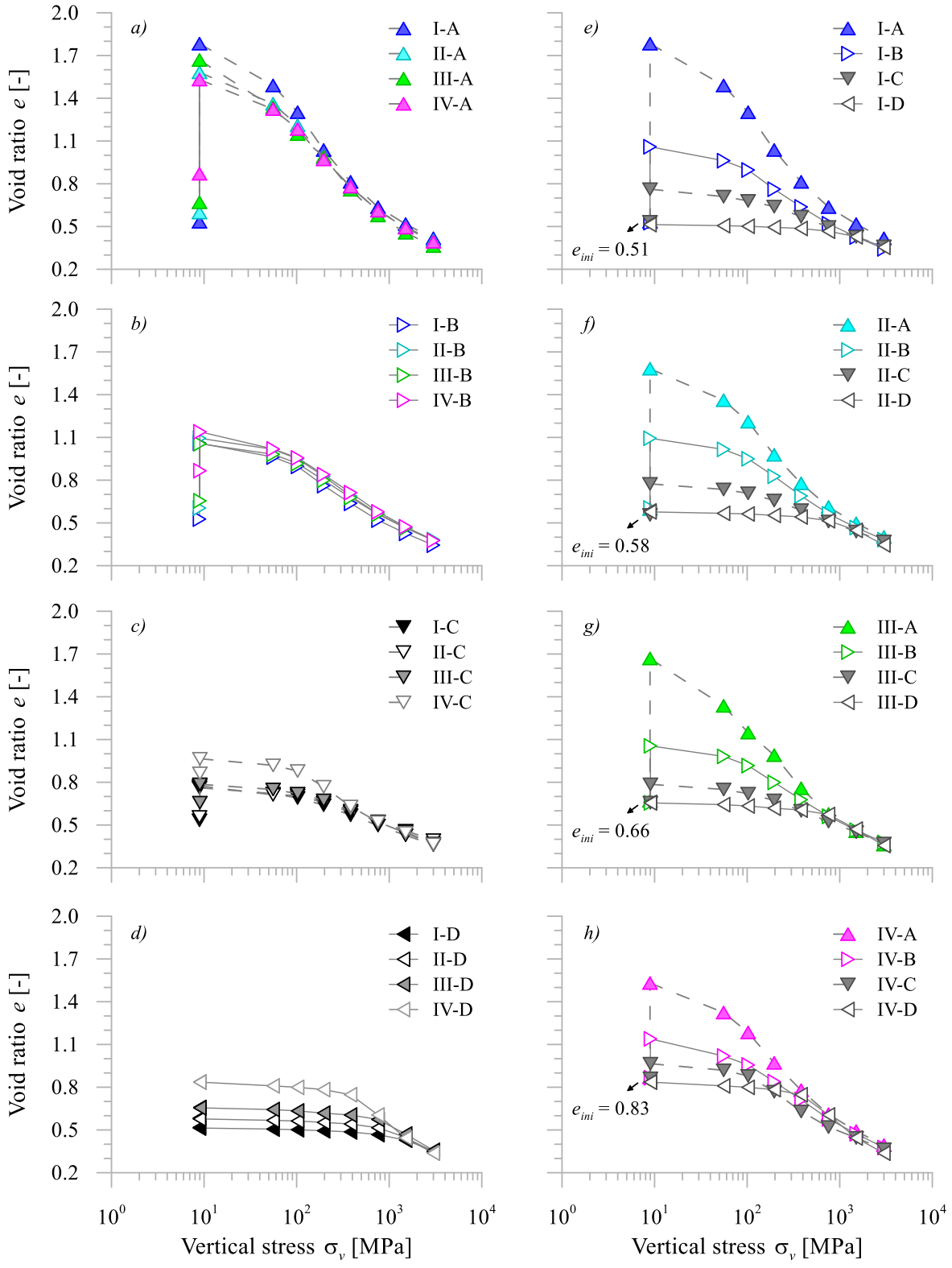

Fig. 6 Results of oedometer experiments conducted on samples characterized by different initial dry densities (Fig. 6 a - d) upon imposing different hydro-mechanical paths (Fig. 6 e - h)

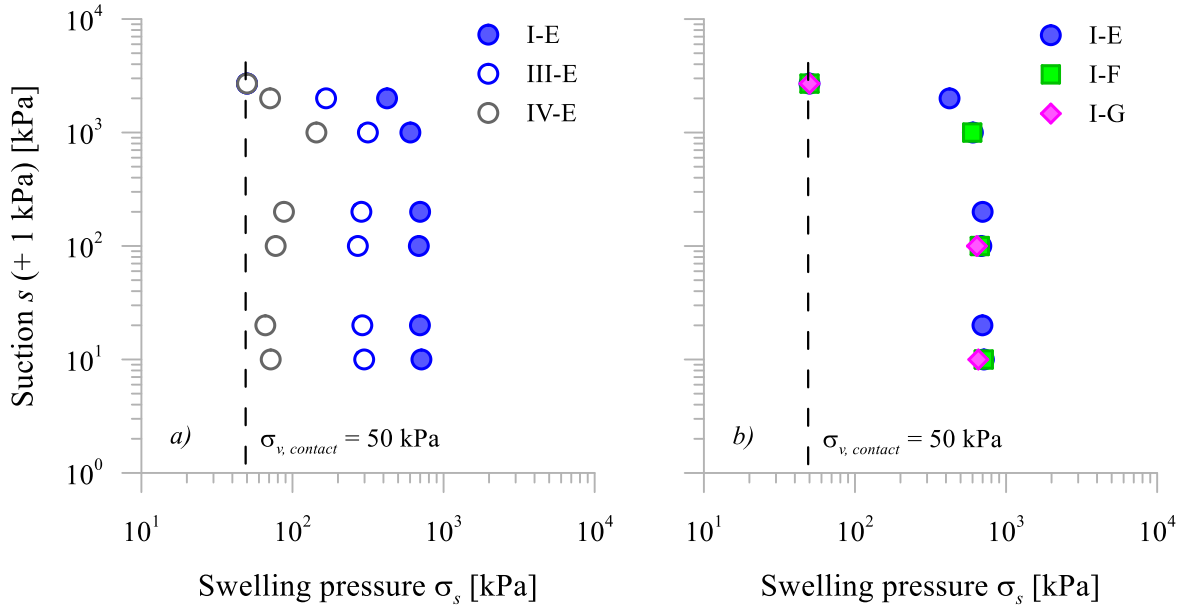

674

675 **Fig. 7** Swelling pressure evolution of a) samples characterized by different initial dry densities upon
676 imposing hydration path E and b) samples characterized by the same initial dry density upon imposing
677 hydration paths E, F, and G

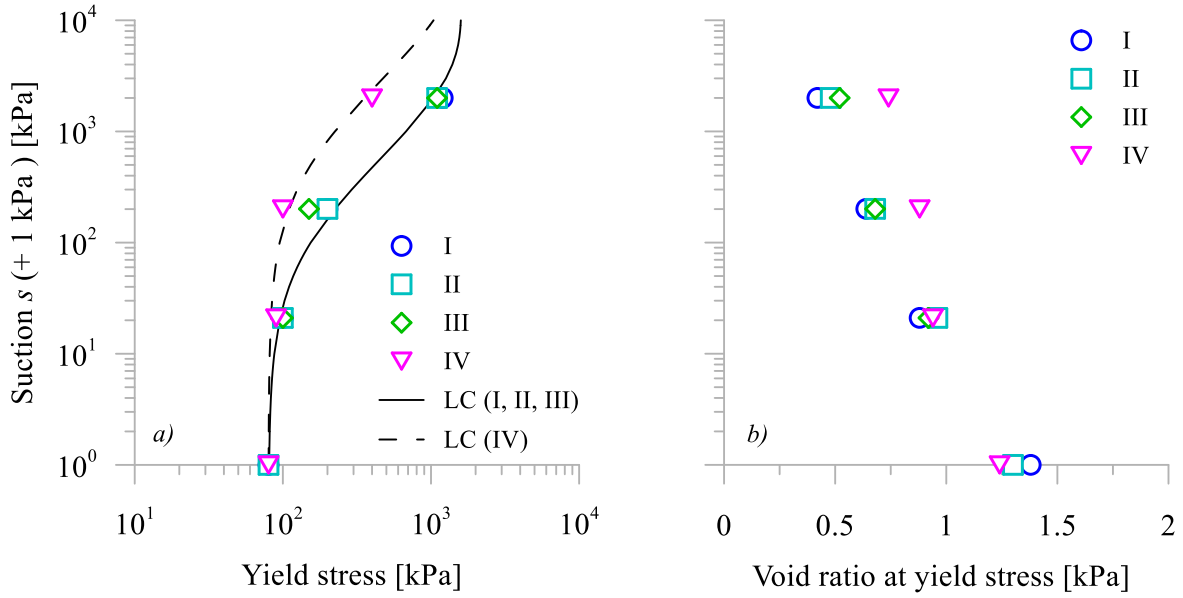

678

679 **Fig. 8** Loading-collapse (LC) curves derived from suction-controlled oedometer experiments

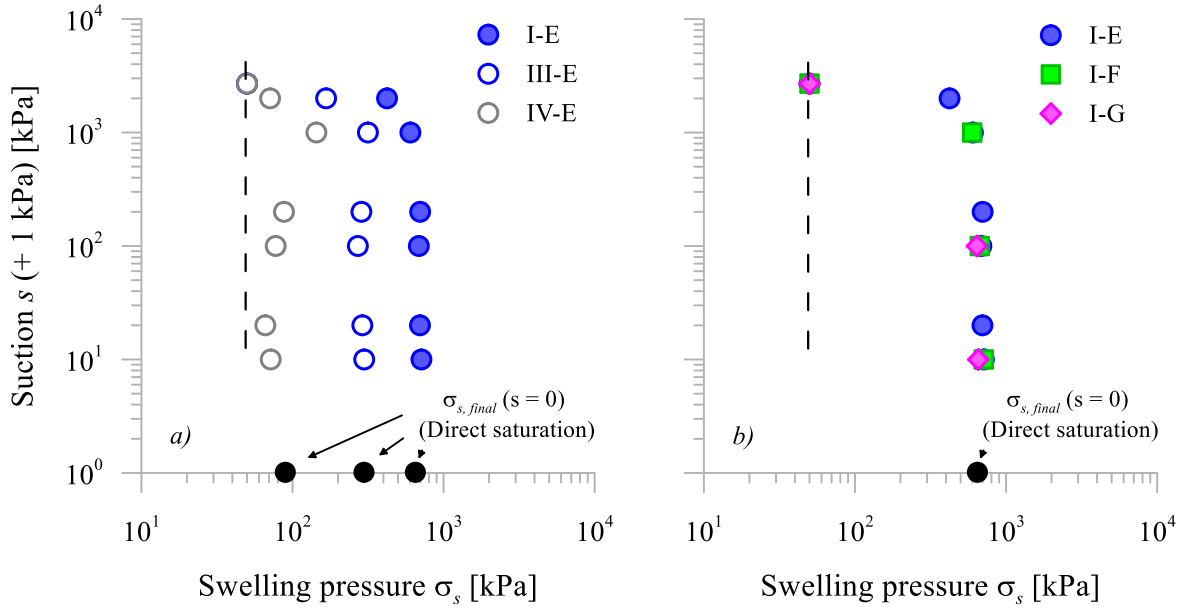

680

681 **Fig. 9** Comparison between the swelling pressure evolution of a) samples characterized by the same
682 initial dry density upon saturating directly and imposing hydration paths E and b) samples upon saturat-
683 ing directly and imposing hydration paths E, F, and G (Values of direct saturation were taken from [19])

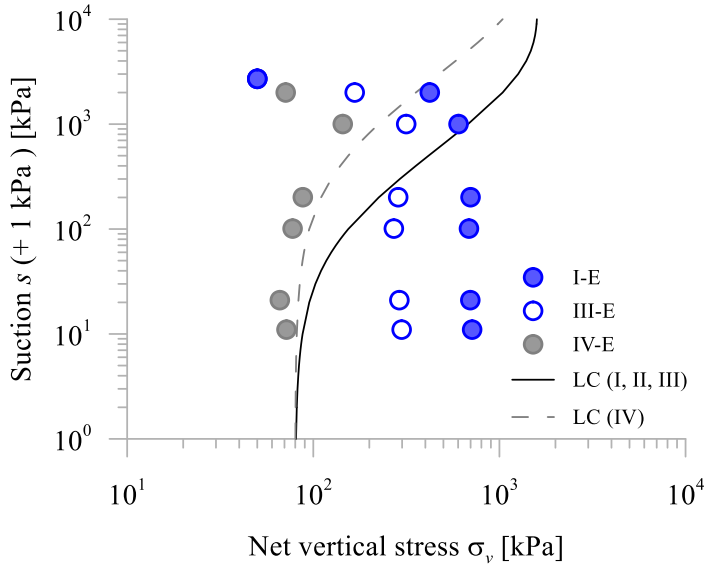

684

685 **Fig. 10** Comparison between LC-curves derived from suction-controlled oedometer experiments and
686 swelling pressure evolution under constant-volume conditions

687 **Table 1** Initial characteristics of samples

Type	Initial dry density	Initial water content	Initial void ratio	Initial porosity	Initial degree of saturation	Initial suction*
	$\rho_{d,\,ini}$	$w_{ini.}$	$e_{ini.}$	$n_{ini.}$	$S_{ini.}$	$s_{ini.}$
	[Mg/m³]	[-]	[-]	[-]	[-]	[kPa]
I	1.72	0.182	0.53	0.35	0.90	2700
II	1.66	0.182	0.59	0.37	0.82	
III	1.59	0.182	0.66	0.40	0.73	
IV	1.44	0.182	0.86	0.46	0.56	

*: measured by means of chilled mirror method

688

689 **Table 2** Experiment program including microstructural and water retention analysis, suction-controlled
690 constant-volume swelling pressure and oedometer experiments

Sample type [1]	Oedometer experiments [2]				Swelling pressure experiments [3]		
	A	B	C	D	E	F	G
I	✓	✓	✓	✓	✓	✓	✓
II	✓	✓	✓	✓			
III	✓	✓	✓	✓			
IV	✓	✓	✓	✓			

[1]: compare Table 1
[2]: Hydro-mechanical paths (compare Fig. 4)
[3]: Hydro-mechanical paths (compare Fig. 5)

691

692